



Efficient wafer-scale poling of electro-optic polymer thin films on soda-lime glass substrates: large second-order nonlinear coefficients and exceptional homogeneity of optical birefringence

Item Type	Article
Authors	Luo, Jingdong; Park, Dong Hun; Himmelhuber, Roland; Zhu, Zong-Long; Li, Ming; Norwood, Robert A.; Jen, Alex K-Y.
Citation	Efficient wafer-scale poling of electro-optic polymer thin films on soda-lime glass substrates: large second-order nonlinear coefficients and exceptional homogeneity of optical birefringence 2017, 7 (6):1909 Optical Materials Express
DOI	10.1364/OME.7.001909
Publisher	OPTICAL SOC AMER
Journal	Optical Materials Express
Rights	© 2017 Optical Society of America.
Download date	26/08/2022 03:26:59
Item License	http://rightsstatements.org/vocab/InC/1.0/
Version	Final published version
Link to Item	http://hdl.handle.net/10150/624966

Efficient wafer-scale poling of electro-optic polymer thin films on soda-lime glass substrates: large second-order nonlinear coefficients and exceptional homogeneity of optical birefringence

JINGDONG LUO,^{1,6} DONG HUN PARK,² ROLAND HIMMELHUBER,³ ZONG-LONG ZHU,¹ MING LI,^{1,4} ROBERT A. NORWOOD,³ AND ALEX K. -Y. JEN^{1,5,7}

¹Department of Materials Science and Engineering, University of Washington, Seattle, WA 98195, USA

²Laboratory for Physical Sciences, University of Maryland, College Park, MD 20740, USA

³College of Optical Sciences, University of Arizona, Tucson, AZ 85721, USA

⁴State Key Lab of Supramolecular Structure & Materials, College of Chemistry, Jilin University, 2699# Qianjin Road, Changchun 130012, China

⁵Department of Physics and Materials Science, City University of Hong Kong, Tat Chee Avenue, Kowloon, Hong Kong SAR, China

⁶jdluo@uw.edu

⁷alexjen@cityu.edu.hk

Abstract: We demonstrate a simple protocol for repeatable and efficient contact poling of guest-host electro-optic (EO) polymer thin films over large areas on soda-lime glass substrates. The poled large-area (up to 13.5 cm²) thin films in this study exhibit very large second-order nonlinear susceptibilities (d_{33} values of 330–520 pm/V) for second-harmonic generation (SHG) and associated large Pockels coefficients (r_{33} values of 105–180 pm/V) at the wavelength of 1.3 μ m. The poling protocol also produced poled EO thin films with excellent optical homogeneity and large positive birefringence with small variation ($\sim 10^{-3}$) of refractive indices over the poled large areas. The study suggests a viable and scalable path towards the realization of integrated photonics based on pre-poled thin films of high performance EO polymers.

© 2017 Optical Society of America

OCIS codes: (000.1570) Chemistry; (190.4710) Optical nonlinearities in organic materials.

References and links

1. S. Bauer, "Poled polymers for sensors and photonic applications," *J. Appl. Phys.* **80**(10), 5531–5558 (1996).
2. L. R. Dalton, P. A. Sullivan, and D. H. Bale, "Electric field poled organic electro-optic materials: state of the art and future prospects," *Chem. Rev.* **110**(1), 25–55 (2010).
3. S. Huang, T. D. Kim, J. Luo, S. K. Hau, Z. Shi, X. H. Zhou, H. L. Yip, and A. K.-Y. Jen, "Highly efficient electro-optic polymers through improved poling using a thin TiO₂-modified transparent electrode," *Appl. Phys. Lett.* **96**(24), 243311 (2010).
4. S. Diahm, S. Zemat, M. L. Locatelli, S. Dinculescu, M. Decup, and T. Lebey, "Dielectric breakdown of polyimide films: Area, thickness and temperature dependence," *IEEE Trans. Dielectr. Electr. Insul.* **17**(1), 18–27 (2010).
5. X. Wang, C. Y. Lin, S. Chakravarty, J. Luo, A. K.-Y. Jen, and R. T. Chen, "Effective in-device r_{33} of 735 pm/V on electro-optic polymer infiltrated silicon photonic crystal slot waveguides," *Opt. Lett.* **36**(6), 882–884 (2011).
6. Y. Enami, C. T. DeRose, D. Mathine, C. Loychik, C. Greenlee, R. A. Norwood, T. D. Kim, J. Luo, Y. Tian, A. K.-Y. Jen, and N. Peyghambarian, "Hybrid polymer/sol-gel waveguide modulators with exceptionally large electro-optic coefficients," *Nat. Photonics* **1**(3), 180–185 (2007).
7. R. Blum, M. Sprave, J. Sablotny, and M. Eich, "High-electric-field poling of nonlinear optical polymers," *J. Opt. Soc. Am. B* **15**(1), 318–328 (1998).
8. J. Luo, S. Huang, Z. Shi, B. M. Polishak, X. H. Zhou, and A. K.-Y. Jen, "Tailored Organic Electro-optic Materials and Their Hybrid Systems for Device Applications," *Chem. Mater.* **23**(3), 544–553 (2010).
9. S. Huang, J. Luo, Z. Jin, M. Li, T. D. Kim, A. Chen, and A. K.-Y. Jen, "Spontaneously poling of electro-optic polymer thin films across a 1.1-mm thick glass substrate by pyroelectric crystals," *Appl. Phys. Lett.* **105**(18), 183305 (2014).

10. S. Huang, J. Luo, Z. Jin, X. H. Zhou, Z. Shi, and A. K.-Y. Jen, "Enhanced temporal stability of a highly efficient guest-host electro-optic polymer through a barrier layer assisted poling process," *J. Mater. Chem.* **22**(38), 20353–20357 (2012).
11. C. C. Teng and H. T. Man, "Simple reflection technique for measuring the electro-optic coefficient of poled polymers," *Appl. Phys. Lett.* **56**(18), 1734–1736 (1990).
12. D. H. Park, C. H. Lee, and W. N. Herman, "Analysis of multiple reflection effects in reflective measurements of electro-optic coefficients of poled polymers in multilayer structures," *Opt. Express* **14**(19), 8866–8884 (2006).
13. R. H. Page, M. C. Jurich, B. Reck, A. Sen, R. J. Twieg, J. D. Swalen, G. C. Bjorklund, and C. G. Willson, "Electrochromic and optical waveguide studies of corona-poled electro-optic polymer films," *J. Opt. Soc. Am. B* **7**(7), 1239–1250 (1990).
14. X. H. Zhou, J. Luo, J. A. Davies, S. Huang, and A. K.-Y. Jen, "Push-pull tetraene chromophores derived from dialkylaminophenyl, tetrahydroquinoliny and julolidiny moieties: optimization of second-order optical nonlinearity by fine-tuning the strength of electron-donating groups," *J. Mater. Chem.* **22**(32), 16390–16398 (2012).
15. D. H. Park and W. N. Herman, "Closed-form Maker fringe formulas for poled polymer thin films in multilayer structures," *Opt. Express* **20**(1), 173–185 (2012).
16. K. D. Singer, M. G. Kuzyk, and J. E. Sohn, "Second-order nonlinear-optical processes in orientationally ordered materials: relationship between molecular and macroscopic properties," *J. Opt. Soc. Am. B* **4**(6), 968–976 (1987).
17. F. Kajzar, K. Horn, A. Nahata, and J. T. Yardley, "Nonlinear optical properties of an organic single crystal: relation between macroscopic and microscopic hyperpolarisabilities," *Mol. Cryst. Liq. Cryst. Sci. Technol., Sect. B: Nonlinear Optics* **8**(3–4), 205–217 (1994).
18. C. C. Teng, M. A. Mortazavi, and G. K. Boudoughian, "Origin of the poling-induced optical loss in a nonlinear optical polymeric waveguide," *Appl. Phys. Lett.* **66**(6), 667–669 (1995).
19. J. C. Burfoot and G. W. Taylor, *Polar Dielectrics and Their Applications* (Macmillan, 1979).
20. T. T. Wang and J. E. West, "Polarization of poly(vinylidene fluoride) by application of breakdown fields," *J. Appl. Phys.* **53**(10), 6552–6556 (1982).
21. A. M. Manea, I. Rau, A. Tane, F. Kajzar, L. Sznitko, and A. Miniewicz, "Poling kinetics and second order NLO properties of DCNP doped PMMA based thin film," *Opt. Mater.* **36**(1), 69–74 (2013).
22. T. Manabe, K. Sato, and T. Ihara, "Measurement of complex refractive index of soda-lime glass at 60 GHz by vector-network-analyser-based scatterometer," *Electron. Lett.* **28**(14), 1354–1355 (1992).

1. Introduction

Efficient poling of high performance electro-optic (EO) polymer thin films at the wafer scale ($>10\text{ cm}^2$) is a key step towards the realization of integrated photonic systems capitalizing on significant performance improvement of these materials [1,2]. However, in common poling protocols of EO polymers, the poled areas are mostly limited to the range of $0.10\text{--}0.50\text{ cm}^2$ in order to obtain consistent results of poled thin film samples in good yields [3]. It remains a great challenge for researchers to further increase the effective poled area. This is largely due to an increase in the probability of finding defects or impurities in thin films leading to dielectric damage under the high poling field [4]. On the other hand, poling of EO polymers in highly confined optical waveguides at the micron- and sub-micron scale remains an outstanding problem in the study of EO polymer processing with respect to achieving reproducible high performance in devices [5, 6]. Therefore, one hurdle that must be overcome is to explore highly repeatable and efficient poling protocols for large area EO thin films. Ideally such protocols can be applied to newly developed high performance EO polymers exhibiting large Pockels coefficients (r_{33} values) greater than 100 pm/V and good stability. Successfully fabricating these pre-poled thin films would potentially accelerate the design and fabrication of optical waveguide devices based on organic EO polymers, and offer unique advantages such as low cost and high optical nonlinearity for integrated photonics research.

Over the past decade, besides the research focus on the molecular design and synthesis of highly efficient organic EO materials, substantial efforts have been made in studying the poling of these materials and their hybrid systems that incorporate dielectric barriers, semi-conductors and conductive polymers [7, 8]. The results suggest that rational design and fabrication of heterogeneous structures is essential to developing highly efficient poling protocols. Further improvement in both poled areas and processing reproducibility is critically dependent on reducing the defect formation and minimizing the probability of dielectric breakdown in order to get highly reliable thermal and electrical properties during poling.

2. Design of contact poling protocols

In this study, we demonstrate a simple protocol for repeatable and efficient contact poling of guest-host EO polymer thin films over large areas. It is a double-layer stack consisting of a micron-thick EO thin film and a millimeter-thick soda-lime glass substrate sandwiched between two electrodes (Fig. 1). Compared to the poling of single-layer EO polymer films, the interposition of a soda-lime glass plate dictates the electrical conductivity of the stack and significantly reduces the probability of electric breakdown of thin film samples under high poling fields. During poling, the relatively high ionic conductivity of soda-lime glass ensures sufficient voltage drop across the EO layer and allows higher applied field strength before breakdown. This design is commensurate with the research efforts in efficient poling of hybrid EO polymer/sol-gel waveguides, and is further inspired by spontaneous pyroelectrical poling of EO polymer thin films across a 1.1-mm thick borofloat glass plate [9]. The direct use of commercial soda-lime glass plate combines high electrical conductivity with excellent thermal and mechanical properties and eliminates multiple steps of material processing in previous studies, thereby encompassing the key aspects related to efficient poling of large area thin films. As a result, the poled large-area (up to 13.5 cm²) thin films exhibit very large second-order nonlinear susceptibilities (d_{33} and d_{31}) and r_{33} values with highly uniform optical birefringence over nearly the entire poled area. The exceptional linear and nonlinear optical properties of large-area thin films through this poling protocol suggest a viable and scalable path towards the realization of integrated photonics based on pre-poled thin films of high performance EO polymers.

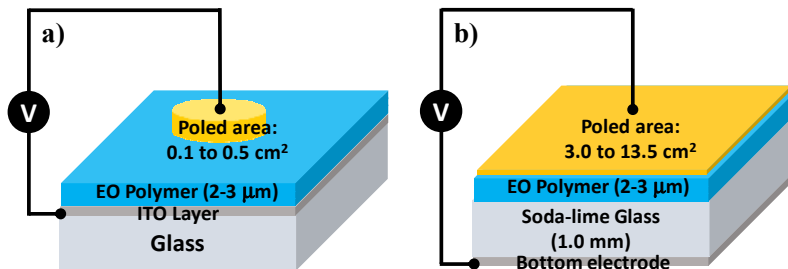


Fig. 1. (a) Standard poling of a single layer EO polymer film sandwiched between two electrodes; (b) Large-area poling design of this study using a double-layer stack consisting of a micron-thick EO thin film and a millimetre-thick soda-lime glass substrate sandwiched between ITO electrode and gold electrode (marked in yellow).

3. Materials and experiments

The EO polymer in this study is a simple guest-host system by doping 15 wt% of a dipolar polyene chromophore AJLZ53 into a random copolymer poly(styrene-*co*-methyl methacrylate) (hereafter AJLZ53/P(S-*co*-MMA)) [10]. To prepare single layer sandwiched thin films as shown Fig. 1(a), the formulated EO polymer solutions with solid content of 6.3 wt% in dibromomethane were filtered through a 0.2-μm PTFE filter and spin-coated onto indium tin oxide (ITO) glass substrates. The films were baked in a vacuum oven at 60 °C overnight, and the film thicknesses were measured to be in the range 2.30–2.80 microns by a Dektak stylus surface profilometer. Then, a thin layer (~100 nm) of gold was sputtered onto the films as a top electrode for contact poling, in which shadow masks were used to define round electrode areas of 0.1 cm² and 0.50 cm², respectively.

Using the gold electrode as the positive terminal, poling voltages corresponding to the field strengths varying from 51 to 128 V/μm were applied to the sandwiched films by a Keithley 237 high voltage source. Leakage currents were monitored by a Keithley 617 Electrometer. The samples were heated from 40 °C to its glass transition temperature (T_g) of

110 °C at the rate of 10 °C/min on a hot stage. After poling, the poled samples were cooled down to room temperature for further analysis and measurement.

Similarly, the bilayer samples shown in Fig. 1(b) were prepared following the processing protocol described above, except for replacing the ITO glass with soda-lime glass slides (Corning code no. 0215 supplied by Ted Pella Inc., thickness of 0.9–1.1 mm; or polished float glass from Delta Technologies, 0.7-mm thick) and increasing the gold electrode area to 3.0–13.5 cm². The selected glass substrates have reliable electrical and mechanical properties for the poling experiments. A fast-drying silver paint was used for the bottom electrode coating on the back side of soda-lime glass, and an unmetallized border was left to avoid flashover around the edges during poling. Typical applied voltages for the poling of bilayer samples ranged from 900 V to 1350 V, depending on the measured resistances of glass slides and EO polymer films to be discussed below. Except for the step of gold sputtering, our experiments were all carried out in laboratory conditions without the use of glove boxes and clean rooms.

The r_{33} values of poled single-layer films were measured at the wavelength of 1.3 μm using a modified Teng-Man reflection technique with error correction [11, 12]. A selected thin ITO electrode with low reflectivity and good transparency was used in order to minimize the contribution from multiple reflections. A transmission type Maker fringe experiment was conducted to evaluate the second-order nonlinear susceptibilities (d_{33} and d_{31} values) at the fundamental wavelength of 1.3 μm for the poled films. For index measurement of all the poled films made using a Metricon 2010 prism coupler, the top gold electrode of the poled films was removed by standard gold etchant.

4. Result and discussion

4.1 Linear and nonlinear optical properties of poled EO films

Table 1. Poling result summary of EO polymer AJLZ53/P(S-co-MMA).

Sample Entry	Configuration, Poled area ^a	Poling field (V/μm)	Leakage current at T_g (A/cm ²)	r_{33} value at 1.3 μm (pm/V)	n_{TE}/n_{TM} at 1.3 μm	Order parameter (Φ)
1	-	-	-	0	1.592/1.590	-
2	SL, 0.5 cm ²	51	1.4×10^{-8}	50	1.590/1.602	0.040
3	SL, 0.5 cm ²	77	8.1×10^{-8}	74	1.586/1.615	0.094
4	SL, 0.5 cm ²	100	8.8×10^{-7}	101	1.583/1.632	0.154
5	SL, 0.5 cm ²	128	3.0×10^{-5}	125	1.580/1.653	0.219
6	DL, 3.2 cm ²	115*	5.3×10^{-6}	110 [†]	1.581/1.642	0.188
7	DL, 13.5 cm ²	110*	-	105 [†]	1.581/1.636	0.172

Note: ^aSL, single-layer of EO thin films; DL, double layer of EO thin film and soda-lime glass plate; *Poling fields were estimated by comparing the resistivity of soda-lime glass and EO polymer films as discussed in the text; [†] r_{33} values extrapolated from the order parameters of poled samples.

As shown in Table 1, the poled single-layer films exhibited large EO activity with an r_{33} -field slope of 1.0 (nm/V)², which is among the highest values for guest-host polymers with the same level of chromophore loading. Notably the positive optical birefringence and r_{33} values of poled films increased significantly with the poling fields. The order parameters can be calculated from measured refractive indices and used as a measure of chromophore alignment in the film. A Sellmeier fit of refractive indices was conducted on two measured index values at 1.3 μm and 1.55 μm using a simple model of absorption and dispersion, in which the refractive index is assumed to have contributions from a non-resonant background n_0 and the two-level charge transfer resonance at frequency ν_0 [13]. Thus for the AJLZ53/P(S-co-MMA) with absorption maximum at 834 nm (or at the frequency ν_0 of 11990 cm⁻¹), we have

$$n = n_0 + A/(11990^2 - \nu^2) \quad (1)$$

A non-resonant refractive index n_0 of 1.493 and a resonance constant A of 8.38×10^6 were obtained. The order parameter for poled films is given by [13]

$$\Phi = (\delta_{TM} - \delta_{TE}) / (\delta_{TM} + 2\delta_{TE}) \quad (2)$$

where $\delta_{TM} = n_{TM} - n_0$ and $\delta_{TE} = n_{TE} - n_0$. The obtained results for the order parameters are given in Table 1 and agree well with those of poling-induced absorbance changes in thin films [14]. Since the refractive indices are measured at wavelengths away from the main absorption peak of the chromophore, this characterization technique could be more reliable than the absorbance measurement in evaluating the poling efficiency of poled films. The quantitative correlation between the order parameters and r_{33} values suggests that the poled large area films on soda-lime glass possessed large r_{33} values of 110 to 115 pm/V.

To further characterize the NLO properties of bilayer structures, a transmission type Maker fringe experiment was conducted to evaluate the second-order nonlinear susceptibilities (d_{33} and d_{31} values) at the fundamental wavelength of 1.3 μm for the poled double layer of EO film on glass [15]. Very large d_{33} values of 330 ± 30 pm/V and a d_{33}/d_{31} tensor ratio of 3.1 were obtained for the sample entry 6 in Table 1. Using the two-level model, the corresponding r_{33} value was estimated to be 145 ± 20 pm/V at 1.3 μm , where the large error bound results from imprecise knowledge of local field and dispersion factors [16]. The differences between r_{33} and d_{33} results could be due to two-photon resonance in SHG and/or Fourier transform definition of optical electric field [17]. Nevertheless, these results of large d_{33} values further verified the high poling efficiency for the poled double layer samples.

4.2 Poling profile and optical quality of poled films

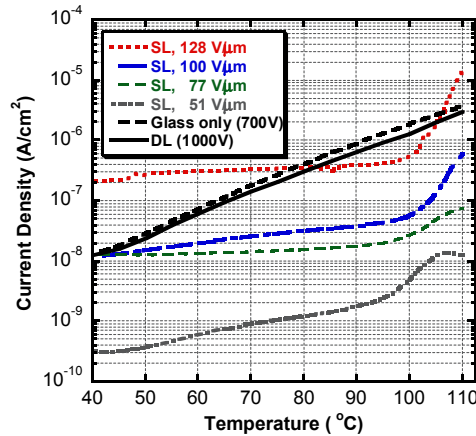


Fig. 2. Current density versus temperature plots for different poled samples of AJLZ53/P(S-co-MMA). The current profile of Corning's soda-lime glass (1.0-mm thick) was provided for comparison.

We did find, however, significant differences in the leak-through current (LTC) and optical quality of poled samples from the two poling configurations. At temperatures close to T_g , the LTC of single-layer films showed the characteristic spike under high poling fields just prior to dielectric breakdown of the polymer film (Fig. 2). Despite the fact that all poled single-layer samples of this study showed sufficiently good quality for optical (refractive index) and NLO (EO and SHG) characterization, high field poling indeed produced a few localized damage spots under the careful examination of optical microscopy (Fig. 3(a)). These defects at the sub-micron to micron scale were not present in unpoled films, and can be attributed to a few irreversible breakdown craters with gold residues and self-healing craters [4]. We think the generation of these localized damages is from the high-field thermal poling process that can

lead to the amplification of pre-existing sites of defects or impurities in the films. Such defects can contribute to high poling-induced optical loss in waveguides [18].

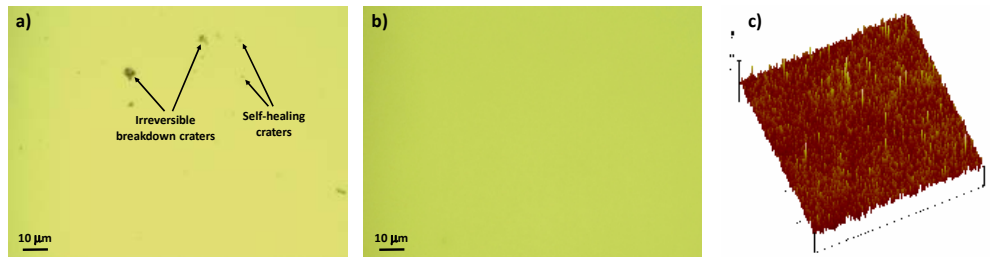


Fig. 3. (a) Breakdown craters observed within the poled single-layer film under optical microscope ($\times 100$), sample entry 4 in Table 1; (b) Image of high film quality under optical microscope ($\times 100$), and (c) Tapping mode AFM topograph of surface for the poled large area film on soda-lime glass (RMS = 0.85 nm), sample entry 6 in Table 1.

In contrast to the behavior of the LTC in single layer structures, the poled bilayer stack of EO polymer film on glass gave a steady pseudo-linear increase of LTC from 40 °C to 110 °C, and no current spikes were observed. The microscope images of poled large area films showed excellent film quality with low surface roughness that are essentially the same as unpoled ones (Figs. 3(b) and 3(c)). These results indicate that electronic thermal stability of the poled thin film in the bilayer structure has been greatly improved to prevent the formation of poling-induced craters or defects.

Comparing the LTC curves of the bilayer with that of soda-lime glass indicates that ionic conduction of the soda-lime glass plate is the dominate conduction mechanism. At 110 °C we measured a relatively constant resistivity of 1.7×10^9 – 2.0×10^9 $\Omega\cdot\text{cm}$ for Corning's 1.0-mm thick soda-lime glass in the applied voltage range from 700 V to 2 kV. The resistivity of the EO films was found to be highly dependent on the applied field, ranging from 1.02×10^{13} $\Omega\cdot\text{cm}$ at 77 V/ μm , 1.65×10^{12} $\Omega\cdot\text{cm}$ at 100 V/ μm , and 8.50×10^{10} $\Omega\cdot\text{cm}$ at 128 V/ μm , respectively, which are about one to three orders of magnitude higher than that of soda-lime glass. This analysis suggested that a more optimal poling condition can be achieved using bilayer stacks and selecting suitable thicknesses for the two layers, because the ratio of the voltage drops across the EO film and the glass plate is proportional to their resistances. For example, according to the resistance analysis, for sample entry 6 in Table 1, ~ 300 V out of total applied 1.0 kV was dropped to the EO layer with thickness of 2.60 μm , resulting in a high poling field strength of 115 V/ μm and a large r_{33} value of 115 pm/V. The interposing of a soda-lime plate also acts as a barrier with a constant resistance, and effectively prevents the surge of LTC just prior to possible dielectric breakdown [10].

One of the more intriguing findings from our study is the exceptional optical homogeneity for the large poled area of thin films on soda-lime glass. The sample entry 7 in Table 1, with effectively poled area of 13.5 cm^2 , gave a very small variation (less than 0.002) of refractive indices over the nearly entire ($> 90\%$) sample area except the edges. This result is extraordinary for a highly birefringent AJLZ53/P(S-co-MMA) films exhibiting extremely sensitive poling-field-dependent properties. It reiterates the key feature of using soda-lime glass for the poling: 1) high ionic conductivities of soda-lime glass ensure sufficient voltage drop and a self-equilibrated applied field strength to the layer of EO thin films; 2) due to its low lateral conductivity, only charges in the immediate vicinity of the defect sites can leak through [13]. This localizing effect significantly reduces the probability of electrical breakdown and the amplification effect from the defects, leading to a highly uniform and efficient poling process for the large-area films.

4.3 Poling of a more efficient high T_g EO polymer

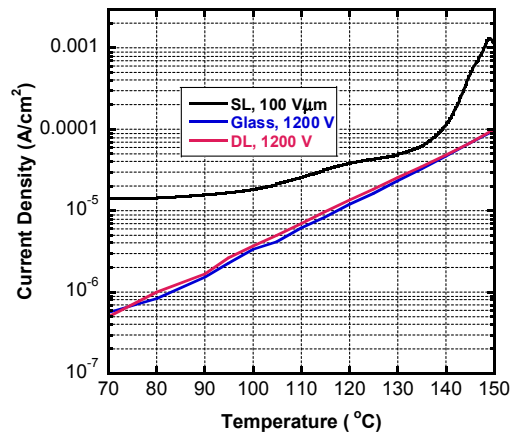


Fig. 4. Current density versus temperature plots for poled samples of AJLZ53/APC in single and double layer structures. Film thickness of the EO polymer was at 1.70–1.80 μm . The current density profile of soda-lime glass (0.7-mm thick) is provided for comparison.

We further applied this double-layer poling configuration to a more efficient polymer, which was formulated by doping 35 wt% of AJLZ53 into amorphous polycarbonate (APC) [10]. The polymer composite has a high T_g of 150 $^{\circ}\text{C}$, and exhibited exceptional combination of large r_{33} values up to 160–180 pm/V at 1.3 μm and good alignment stability at 85 $^{\circ}\text{C}$. By following the similar protocol of sample preparation and poling process, we were able to pole it efficiently on a polished 0.7-mm thick soda-lime glass with the poled area of 3.6 cm^2 , and we obtained an ultralarge d_{33} value of 520 ± 30 pm/V and an associated r_{33} value of 180 ± 25 pm/V at 1.3 μm . Similar to the AJLZ53(15%)/P(S-co-MMA) discussed earlier, the poled films of AJLZ53(35%)/APC displayed large positive birefringence and high optical homogeneity with n_{TE}/n_{TM} of 1.706/1.768 at 1.3 μm and n_{TE}/n_{TM} of 1.670/1.716 at 1.55 μm , respectively. Besides high poling efficiency, we also recorded a steady pseudo-linear increase of LTC for the poled double layer sample, which was an order of magnitude lower than that of poled single-layer films (Fig. 4). This improvement in controlling the LTC was achieved by inserting the soda-lime glass for the poling of a highly efficient but more conductive EO polymer.

5. Conclusions

Poling is an important step in determining the processing scalability and performance of polar dielectric materials. In comparison to the poling of other types of polar dielectrics such as ferroelectric crystals, piezoelectric ceramics and ferroelectric polymers [19], it is fair to say that poling of new generation EO polymers has been considered to be a daunting task comprising a complexity of electrical, thermal and mechanical parameters in a process requiring high field strength. In this study, we have demonstrated an efficient wafer-scale poling of EO polymer thin films on soda-lime glass substrates, and achieved large second-order optical nonlinearities with excellent optical homogeneity. It addresses the processing scalability and reliability for the poling of highly efficient EO polymers, which is critically important for the design and fabrication of EO polymer based photonic devices. The applicable poled area of this study was set at 13.5 cm^2 from the bench-top experiments, and we believe it can be further expanded to the scale of 40–80 cm^2 by using larger systems.

In the past, soda-lime glass has been used as an excellent substrate in the corona and contact poling of nonlinear optical (NLO) polymers and ferroelectric polymers [13, 20, 21]. While we have gained much insight from these studies and some of the recent research efforts

in using a barrier layer to improve the poling of EO polymers, our present study has advantages over previous similar ones because of its simplicity, quantitative control of field strength over a large poled area, short poling time, relatively low applied voltages, no reactive corona ions generated, and little to no dielectric breakdown damages. In addition, we have analyzed the relationship between photonic properties (such as NLO coefficients and optical birefringence) and poling conditions for two representative EO polymers, and their quantitative correlation should be beneficial for the design and fabrication of EO polymer based photonic devices. For high-speed optical modulation and electromagnetic wave sensing, soda-lime glass wafer can be considered as an excellent dielectric substrate exhibiting reasonable complex refractive indices at both radio and optical frequencies [22]. It suggests a viable and scalable path towards the realization of integrated photonic devices based upon highly efficient EO polymer waveguides on the glass substrate. This is an ongoing effort, and further progress will be reported in due course.

Funding

Air Force Research Laboratory (AFRL) and Air Force Office of Scientific Research (AFOSR) (FA8650-14-C-5005), under the Small Business Technology Transfer Research program (STTR).

Acknowledgments

Technical advice from the program managers Dr. Robert L. Nelson and Dr. Charles Y-C. Lee are greatly appreciated. Extra supports are acknowledged for Soluxra LLC (J. L.), Boeing-Johnson Foundation (A. K-Y. J.), and State-Sponsored Scholarship for Graduate Students from China Scholarship Council (M. L.). The authors also thank Dr. Warren N. Herman for providing valuable advice and proof-reading.